

Cluster-Impact Fusion

R. J. Beuhler, G. Friedlander, and L. Friedman

Chemistry Department, Brookhaven National Laboratory, Upton, New York 11973

(Received 9 June 1989)

Deuteron-deuteron fusion, detected via the 3-MeV protons produced, is shown to occur when singly charged clusters of 25 to 1300 D_2O molecules, accelerated to 200 to 325 keV, impinge on TiD targets. The energy and cluster-size dependence of the fusion rate are discussed. The fusion events are shown to originate from the cluster-ion impacts rather than from D^+ or D_2O^+ ions in the beam. The observed rates may be correlated with the compressions and high energy densities created in collision spikes by cluster-ion impacts.

PACS numbers: 79.20.Rf, 25.45.-z, 47.40.Nm, 52.50.Lp

The impact of accelerated cluster ions on solid surfaces has been shown to produce very high transient particle and energy densities.¹ The experiments reported in this Letter show that singly charged, heavy-water cluster ions containing between 25 and 1300 D_2O molecules and accelerated to energies up to 325 keV can, on impact with titanium deuteride targets, generate thermonuclear D-D fusion reactions.

The apparatus used for the experiments is shown schematically in Fig. 1. The ion source and the techniques for mass analysis and for acceleration of water cluster ions have previously been described in detail.² Water molecule ions in helium carrier gas were generated in a corona discharge. The weakly ionized gas mixture was expanded through a nozzle and skimmer into a high-vacuum system. As discussed previously,^{2,3} a combination of mass analysis and careful determination of secondary-electron yields produced by impact of cluster ions on a target suffices to determine the m/e ratios of the ions and to count the number and kind of atoms in the cluster.

The cluster ions prepared by these techniques were

subjected to quadrupole mass analysis² and electrostatic focusing before introduction into a Cockroft-Walton accelerator approximately 1 m long. After acceleration, ions passed through an aperture into a vacuum chamber containing a TiD target of about 1-cm² surface area at $\sim 45^\circ$ to the beam axis and approximately 1.5 cm from a 300-mm² Ortec "ruggedized" silicon solid-state detector. The active surface of the detector was covered with a 50- $\mu\text{g}/\text{cm}^2$ layer of aluminum.

The cluster beam current was monitored by measurement of secondary electrons ejected from the TiD target (i.e., measurement of apparent positive-ion current to the target). Cluster-ion intensity measurements are subject to error when a small fraction of the ions make grazing collisions with the edges of the column exit aperture. Such collisions produce low-mass fragments [e.g., 300-eV deuterons from 300-keV $(D_2O)_{100}$ clusters] that can eject secondary electrons from the target but do not have enough energy to produce D-D reactions. Careful attention to optimization of secondary-electron distributions is required to ensure proper beam focusing, particularly when the beam energy is varied. Relative values of pri-

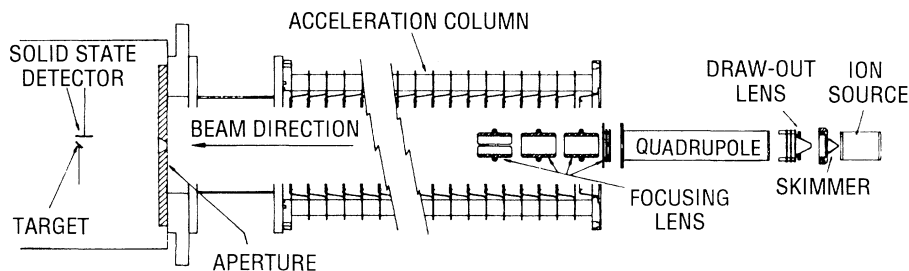


FIG. 1. Schematic diagram of the apparatus. A mixture of D_2O and He gas is ionized in a corona discharge in the ion source and expanded through a supersonic nozzle into a differentially pumped region between nozzle and skimmer. Cluster ions pass through the skimmer, are extracted with 10–50 eV by the draw-out lens, and mass analyzed in the quadrupole mass spectrometer using a low-frequency (~ 292 kHz) power supply. The mass-analyzed ions are focused and then accelerated in a Cockroft-Walton column. Ions traverse an ~ 1 -cm aperture and impact on a TiD target attached to a Keithly picoammeter. A silicon solid-state detector ~ 1 cm from the target is used to measure protons, tritons, and x rays produced by cluster impact on the TiD target.

mary beam intensities were calculated from the measured yields of secondary electrons, using data obtained previously.⁴ Cluster beam intensities were in the range of 10^{-8} – 10^{-9} A.

The primary signature of D-D fusion used in this experiment was the detection of 3.0-MeV protons from the reaction ${}^2\text{H} + {}^2\text{H} \rightarrow {}^1\text{H} + {}^3\text{H}$ which is exoergic by 4.0 MeV. A typical spectrum obtained with a silicon detector near a TiD target bombarded with $(\text{D}_2\text{O})_n^+$ ions is shown in the top half of Fig. 2. [The ions are presumably $(\text{D}_2\text{O})_n\text{D}^+$ but our mass resolution is insufficient to establish this point. For simplicity we refer to the cluster ions as $(\text{D}_2\text{O})_n$ or $(\text{D}_2\text{O})_n^+$.] The detector was calibrated with α particles from ${}^{241}\text{Am}$ (5.48 MeV) and ${}^{148}\text{Gd}$ (3.18 MeV). The detector output data were digitized, and converted to light pulses in the high-voltage terminal. The light pulses were transported on fiber-optic cables to ground potential. The maximum data rate of this system was $\sim 10^5/\text{s}$. Considerable summing of pulses or pulse pileup of x rays was noted and is shown in the first 80 channels of the Tracor-Northern multi-channel-analyzer display presented in Fig. 2. Just beyond the tail of these pileup pulses, in channels 90–140, is a broad peak, presumably due to 1-MeV tritons. The ${}^3\text{He}$ ions expected from the reaction ${}^2\text{H} + {}^2\text{H}$

$\rightarrow {}^3\text{He} + n$, degraded to about 0.75 MeV by the Al layer on the detector, are not observed. They may be obscured by the x-ray background. The broadening of the peaks presumably arises from the ions passing through the Al layer on the detector at various angles. Confirmation of the assignments of the ${}^1\text{H}$ and ${}^3\text{H}$ peaks was obtained by insertion of a 4.8-mg/cm² Al absorber between target and detector. The spectrum so obtained is shown in the lower part of Fig. 2, with the proton peak shifted down by 0.3 MeV and the ${}^3\text{H}$ peak shifted into the x-ray background, as expected for that absorber thickness. Many spectra like those in Fig. 2 were taken, with different cluster sizes and accelerating voltages. Counting rates were low but the signals were well above any background noise as long as acceleration column voltages were maintained at less than 325 kV.

No 3-MeV protons were observed when the D_2O clusters were replaced by H_2O clusters, nor when D_2O clusters were incident on hydrogen-loaded rather than deuterium-loaded titanium.

Figure 3 shows the dependence of the reaction rate on cluster size at a given accelerating voltage (300 kV in this case). In the range of 100–500 D_2O 's per cluster there is a broad maximum in the reaction rate, with falloff toward both smaller and larger clusters; at the extremes investigated, $(\text{D}_2\text{O})_{25}$ and $(\text{D}_2\text{O})_{1300}$, the rate was about 5 and 10 times smaller, respectively, than at the maximum. Taking the detector geometry into account, the fusion rates for 100–500 D_2O clusters at 300 keV are $\sim 0.05 \text{ s}^{-1}$ per cluster nA.

The energy dependence of the reaction rate is shown for $(\text{D}_2\text{O})_{150}$ clusters in Fig. 4. The rate is seen to increase by about an order of magnitude between 225 and 300 keV.

Both the cluster-size dependence and the energy dependence are strong arguments for fusion indeed being

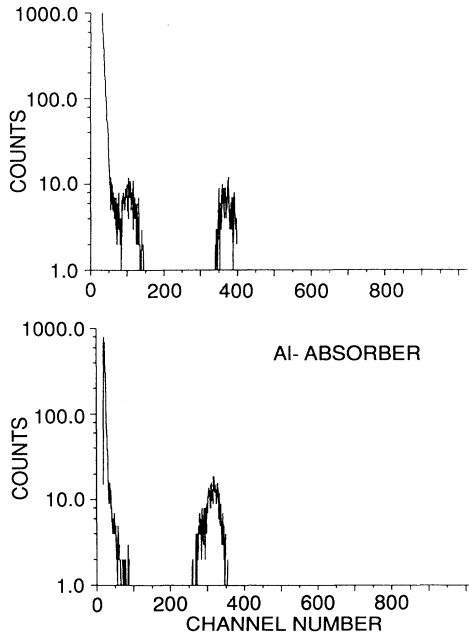


FIG. 2. Evidence for fusion is presented (in the upper figure) through observation of peaks at ~ 3 and ~ 1 MeV corresponding to D-D fusion products. When a 4.8-mg/cm² Al absorber is placed between the TiD target and the solid-state detector, the triton peak is shifted (lower figure) into the x-ray background and the proton peak is shifted down by ~ 300 keV. The energy scale is calibrated with a value of 8 keV/channel.

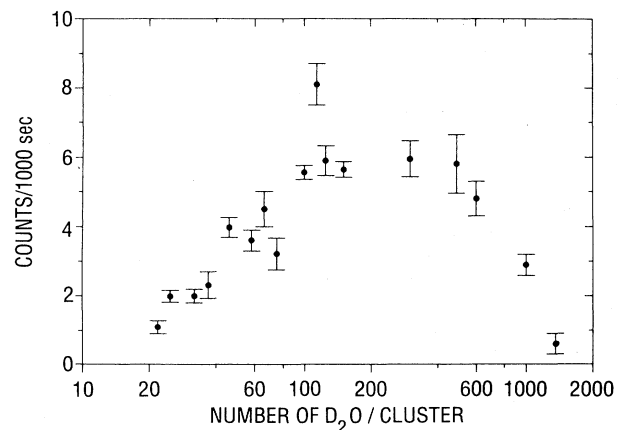


FIG. 3. Dependence of proton yield on cluster size at 300-kV accelerating potential. The ordinate scale is proton counts per 1000 s per nA of cluster current.

caused by impact of cluster ions, rather than by small-ion contaminants in the beam. The observed energy dependence between 200 and 300 keV is very much steeper than that for deuterons over this energy range, so that deuterons originating in the source cannot be responsible for the observed fusions. If D_2O^+ ions produced by collision-induced dissociation of clusters or by ionization of background water vapor in the flight path were responsible for the fusion events, the decrease in rate with increasing cluster size would be hard to rationalize; with increasing cluster size more water is introduced in the vacuum system and collision-induced dissociation increases.

Only ions carefully focused prior to acceleration will traverse the aperture at the end of the column and enter the target chamber. Consequently, products of electron impact (from backstreaming electrons) on residual gas in the column or collision-induced dissociation of cluster ions in the column are not expected to be transmitted through the exit aperture with any appreciable efficiency. However, products of electron-impact ionization of residual gases or collision-induced dissociation of clusters between the exit of the quadrupole and the focusing lens stack can be collected in the target chamber with the full acceleration of the column. These species may operate as beam contaminants and produce fusion reactions.

Definitive evidence for the conclusion that the fusion events are produced by cluster-ion impacts was provided by experiments in which a silicon surface-barrier detector was placed directly in the ion beam. To limit the direct impacts on the detector, the beam was attenuated by a factor of 65 by means of a 0.027-in. aperture in a beam stop placed in front of the detector. With cluster

beams containing 130 D_2O molecules per cluster and accelerated to various energies between 250 and 325 keV, no peak at or near the full beam energy was found, thus excluding the possibility of full-energy D^+ ions hitting the target. The Al film on the silicon detector is thick enough to prevent $(D_2O)_{130}$ clusters from depositing most of their energy in the detector. On impact, such clusters would presumably break up into their constituents, none of which would have sufficient energy to penetrate the Al layer. If D_2O^+ (or OD^+) ions are present in the beam, they too will break up on impact; tabulated electronic stopping powers for O and D ions⁵ indicate that the energy deposition after passage through $50 \mu\text{g}/\text{cm}^2$ Al should be at least 150 keV below the full beam energy. The contribution of nuclear stopping makes the expected energy deficit even slightly greater. No such peak was observed; instead, a small peak always appeared approximately 100 keV below full beam energy. This is consistent with the energy loss expected for fully accelerated He^+ ions in the Al layer, and He^+ might indeed be expected in the beam from the He carrier gas. When Ne was substituted for He as carrier gas, the peak 100 keV below the full beam energy disappeared. Instead, a small peak now appeared at the expected position of D_2O^+ (masked in the He experiments in the valley between the x-ray and He peaks). From its magnitude, the ratio of beam intensities in this auxiliary experiment and the main experiment, the geometrical efficiencies, and the known cross sections for deuteron-induced fusion, it was determined that no more than 0.3% of the observed fusion events at 300 kV accelerating voltage are attributable to D_2O^+ impacts.

We conclude that the observed fusion reactions are primarily produced by impact of accelerated cluster ions on the TiD target. Estimates of reaction rates require assumptions on the size of the target volume element heated and compressed by cluster impact. If we assume that only the top ten layers of target atoms are heated and compressed to an extent sufficient for fusion to occur, a crude estimate of 1000 is obtained for the number of D atoms in the critical volume, when a spherical $(D_2O)_{100}$ cluster accelerated to 300 keV impinges on a TiD lattice (face-centered cubic lattice with unit cell dimension 4.48 Å). We correct the measured yield of $\sim 0.005 \text{ s}^{-1}$ per nA of $(D_2O)_{100}$ for the limited acceptance of the detector. The corrected yield of $\sim 0.05 \text{ s}^{-1}$ per nA of $(D_2O)_{100}$ cluster ions corresponds to approximately 10^{-14} events/deuteron. With a confinement time taken to be $\sim 10^{-13} \text{ s}$, the yield is roughly 10^{-1} s^{-1} , an extraordinarily high value. The fusion rate in $\text{cm}^{-3} \text{ s}^{-1}$ is given by $R = \eta^2 \bar{\sigma} \bar{v}$.⁶ η is the deuteron number density, $\bar{\sigma}$ is the cross section, and \bar{v} is the deuteron velocity averaged over the velocity distribution in the collision spike. σ is given by $\sigma(E) = S(E)/Ee^{-31.28/E^{1/2}}$, where E is in keV and $S(E)$ (Ref. 7) is derived from independent data on higher-energy D-D reactions. By assuming no compression occurs the experimental results lead to a

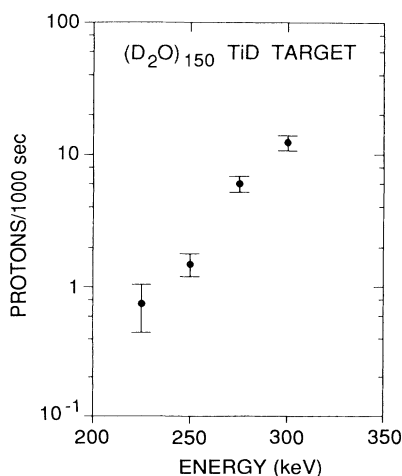


FIG. 4. Preliminary study of the energy dependence of the observed D-D reaction using clusters containing 150 D_2O molecules. The ordinate scale is protons per 1000 s per nA of cluster current.

value of σ more than 10 orders of magnitude larger than that computed for 300-eV D impacts using the standard value of $S(E) = 55 \times 10^{-24} \text{ cm}^2 \text{ keV}$.

We have no detailed model for the complex processes taking place in our experiment. We note that the rate equation above indicates the need to consider *both* compression and heating in these fusion reactions. This would help somewhat to explain the results with light-water clusters mentioned above and the steep energy dependence of yield in Fig. 4. However, the magnitude of the calculated rate is not easily explained by the number-density term above in the rate equations. We can only speculate on the conjecture that motivated the initiation of these experiments. We assumed that theoretical results on the effect of compression on rates of fusion of diatomic oscillators^{8,9} were relevant to what might be observed with a polyatomic oscillator system in an inertially confined collision spike.

The compression of dense matter by shock waves is known to operate as a one-dimensional strain, with changes in internuclear distances in the shocked material, initially, almost exclusively along the direction of the shock.¹⁰ The resulting decreases in internuclear distance along the shock axis can be expected to scale roughly with the reciprocal of density changes rather than with the reciprocals of their cube roots.

Pressures exerted by $(\text{D}_2\text{O})_{100}$ cluster ions with 300 keV initial kinetic energy impacting on an area of $\sim 10^{-14} \text{ cm}^2$ can be very roughly estimated from stopping-power energy losses. If we take 100 eV for the energy loss per water molecule in the top atomic layer of TiD, the deceleration of the $(\text{D}_2\text{O})_{100}$ projectile traversing that layer as a one-dimensional disk is estimated to produce a pressure of about 80 Mbar. Calculations of densities of deuterium compressed in much weaker shocks by pressures an order of magnitude less than 80 Mbar give values of about 0.8 g/cm^{-3} ,¹¹ ~ 5 times the density of liquid D_2 under normal pressure. The transient compression and heating associated with impact of 300-keV $(\text{D}_2\text{O})_{100}$ clusters suggested the possibility of

the generation of conditions that would provide very large increases in fusion rates.

The experiments reported here provide a novel approach to the study of fusion reactions in dense assemblies of reactant atoms. The high fusion rates and the sensitivity to projectile energy suggest the possibility of a possible new path to fusion power.

The preparation of titanium hydride and titanium deuteride targets by W. Kunnmann is gratefully acknowledged. We are grateful to J. Weneser for helpful discussions. This research was carried out at Brookhaven National Laboratory under Contract No. DE-AC02-76CH00016 with the U.S. Department of Energy and supported by its Division of Chemical Sciences, Office of Basic Energy Sciences.

¹See, e.g., R. Beuhler and L. Friedman, *Chem. Rev.* **86**, 521 (1986).

²R. J. Beuhler and L. Friedman, *J. Chem. Phys.* **77**, 2549 (1982).

³R. J. Beuhler and L. Friedman, *Int. J. Mass Spectrom. Ion Phys.* **23**, 81 (1977).

⁴R. J. Beuhler and L. Friedman, *J. Appl. Phys.* **48**, 3928 (1977).

⁵L. C. Northcliffe and R. F. Schilling, *Nucl. Data Tables A* **7**, 268 (1970); **7**, 272 (1970).

⁶D. Keefe, *Ann. Rev. Nucl. Sci.* **32**, 394 (1982).

⁷D. D. Clayton, *Principles of Stellar Evolution* (McGraw-Hill, New York, 1968), p. 294.

⁸S. E. Jones, E. P. Palmer, J. B. Czirr, D. L. Decker, G. L. Jensen, J. M. Thorne, S. F. Taylor, and J. Rafelski, *Nature (London)* **338**, 737 (1989).

⁹S. E. Koonin and M. Nauenberg, *Nature (London)* **339**, 690 (1989).

¹⁰M. H. Rice, M. G. McQueen, and J. M. Walsh, *Solid State Physics* (Academic, New York, 1958), Vol. 6, pp. 11 and 12.

¹¹L. Friedman and G. Vineyard, *Comments At. Mol. Phys.* **15**, 251 (1984).